NANOSYSTEMS:
PHYSICS, CHEMISTRY, MATHEMATICS

Gajtko O.M., et al. *Nanosystems: Phys. Chem. Math.*, 2025, **16** (3), 343–351.
http://nanojournal.ifmo.ru
DOI 10.17586/2220-8054-2025-16-3-343-351

Original article

Epoxide-mediated synthesis of germania aerogels in acetic acid

Olga M. Gajtko[a], Svetlana V. Golodukhina[b], Sergey Yu. Kottsov[c], Alexandra G. Son[d],
Taisiya O. Kozlova[e], Alexander E. Baranchikov[f]

Kurnakov Institute of General and Inorganic Chemistry of the Russian Academy of Sciences, Moscow, Russia

[a]olga.gajtko@igic.ras.ru, [b]golodukhina@igic.ras.ru, [c]skottsov@igic.ras.ru, [d]agson@igic.ras.ru,
[e]taisiya@igic.ras.ru, [f]baranchikov@igic.ras.ru

Corresponding author: Olga M. Gajtko, olga.gajtko@igic.ras.ru

PACS 82.70.Gg, 61.46.-w, 81.20.-n

ABSTRACT A novel alkoxide-free method for the sol-gel synthesis of germania aerogels is proposed. The method is based on the hydrolysis of $GeCl_4$ by propylene oxide in concentrated acetic acid which is used as a solvent. The proposed protocol allows one to obtain monolithic amorphous germania aerogels constructed of a three-dimensional network of nanoscale ($\sim$ 20 nm) particles and possessing specific surface area of about 80 m^2/g. The addition of hydrochloric acid to the reaction mixture results in the synthesis of nanocrystalline GeO_2 (hexagonal system) aerogels. The synthesized materials were characterized by X-ray diffraction, IR spectroscopy, scanning electron microscopy and low temperature nitrogen adsorption.

KEYWORDS sol-gel synthesis, germanium dioxide, propylene oxide, supercritical drying

ACKNOWLEDGEMENTS This study is performed within the ARIADNA Collaboration operating under the NICA facility as a part of State Assignment “Solving topical problems with NICA charged particle beams (Ref. # 124110600054-0)”. This research was performed using the equipment of the JRC PMR IGIC RAS.

FOR CITATION Gajtko O.M., Golodukhina S.V., Kottsov S.Yu., Son A.G., Kozlova T.O., Baranchikov A.E. Epoxide-mediated synthesis of germania aerogels in acetic acid. *Nanosystems: Phys. Chem. Math.*, 2025, **16** (3), 343–351.

1. Introduction

Nanodispersed germanium oxide is unique material possessing outstanding thermal, optical and electrical properties. Germanium dioxide is characterised by a large band gap energy (5 eV), high refractive index, intense blue photoluminescence, high reversible capacity and excellent thermal stability [1–3], giving this material a wide range of diverse applications [4–13]. In view of the considerable practical interest, a number of different approaches to synthesising nanostructured GeO_2 have been described in the literature, including gas transport reactions, chemical vapor deposition, electrospinning, sol-gel precipitation, and others [14–21]. The aforementioned methods result in germanium dioxide in the form of dispersed nanoparticles, 1D or 2D structures; however, the methods for the production of ultralight and highly porous GeO_2 aerogels are extremely limited [22–24]. At the same time, the conjunction of the physicochemical properties of GeO_2 with the unique structure of aerogels could result in new functional materials with unusual characteristics, e.g. electrochemical.

Currently, the common method to obtain metal oxide aerogels is the alkoxide-mediated synthesis, which includes the hydrolysis and polycondensation of an alkoxide of the corresponding metal with subsequent drying of a wet-gel. The most typical example of oxide aerogels is silica aerogels, and the wide variety of the methods for their synthesis is extensively presented in literature [25]. Surprisingly, despite the similar chemical properties of silicon and germanium, the synthetic approaches for GeO_2 aerogels are extremely scarse. Presumably, this is due to the markedly higher rate of germanium alkoxide hydrolysis relative to the hydrolysis of silicon alkoxides [26–29]. Thus, special approaches for the synthesis of GeO_2 lyogels should be used. In particular, Kucheyev *et al.* [30] carried out a controlled hydrolysis of germanium methoxide in acetonitrile, followed by a rapid supercritical drying. As a result, aerogel formed consisting of elongated nanoligaments of amorphous GeO_2 which possessed specific surface area of $\sim$60 m^2/g. Zhang *et al.* obtained GeO_2 lyogel using germanium ethoxide dissolved in absolute ethanol and dilute hydrochloric acid as a gelation catalyst [31,32]. GeO_2 aerogels were synthesized upon the supercritical drying of the lyogels, they possessed high degree of crystallinity, specific surface area up to 155 m^2/g and strong blue luminescence.

Due to the high cost of metal alkoxides as well as their high hydrolysis rates, epoxide-mediated method has also been proposed as an alternative for the synthesis of metal oxide aerogels [33,34]. Nevertheless, to the best of our knowledge, the use of this versatile method for the synthesis of GeO_2 aerogels has been documented in only a single report. Briefly, this approach involves the synthesis of amorphous and crystalline germanium dioxide aerogels using a propylene oxide as a hydrolysing agent, aprotic solvents (butyl/ethyl acetate), and hydrochloric acid as a controlled source of protons [35,36].

In the present work, it was hypothesised that acetic acid being a common reagent for the synthesis of metal oxide sol-gel materials [37–42] can also be used for the synthesis of germania aerogels as a solvent and a source of protons.

2. Experimental section

The following materials were used as received: germanium chloride $GeCl_4$ (Acros Organics, 99.99 %), acetic acid (Aldosa, pure grade), hydrochloric acid (Sigma Tec, extra-pure grade), propylene oxide (Thermo Scientific, 99.5 %).

The synthesis scheme is shown in Fig. 1. To obtain germanium oxide lyogels, 0.10 ml (0.87 mmol) of germanium chloride was dissolved in 1 – 4 ml (17.4 – 69.6 mmol) of glacial acetic acid (AcOH). Subsequently, 0.61 ml (8.7 mmol) of propylene oxide (PO) was added to the resulting solution, which was then cooled to ∼ 18 °C. In some cases, up to 0.16 ml (8.7 mmol) of concentrated 36.5 wt. % hydrochloric acid was additionally added to the cooled solution under sonication. The final molar ratios of the components in the reaction mixtures as well as the visual observations are presented in Table 1.

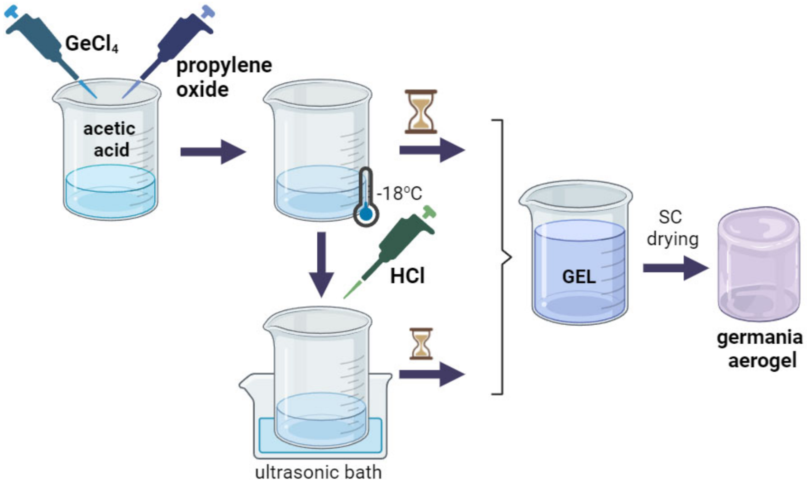

FIG. 1. The scheme of the synthesis of germania aerogels synthesised from the mixtures of $GeCl_4$, acetic acid and propylene oxide as starting reagents

TABLE 1. Designations and synthesis parameters of the germanium oxide aerogels

Sample	Molar ratio $GeCl_4$:AcOH:HCl:PO	Gelation time	Lyogels stability	Supercritical drying
Ac20	1:20:0:10	∼20 days	Monolithic gel ≥ 1 week	+
Ac60	1:60:0:10	∼ 9 days	Monolithic gel ≥ 1 week	+
Ac80	1:80:0:10	∼ 9 days	Monolithic gel ≥ 1 week	+
Ac60_HCl2.5	1:60:2,5:10	∼60 min	Monolithic gel ≥ 1 week	+
Ac60_HCl5	1:60:5:10	∼ 15 min	Monolithic gel ≥ 1 week	+
Ac80_HCl5	1:80:5:10	∼ 120 min	Monolithic gel ≥ 1 week	+

The monolithic lyogels which formed during the synthesis were subjected to supercritical drying, carbon dioxide was used as a solvent. Supercritical drying (SC) in CO_2 was carried out in a setup consisting of a high-pressure pump Supercritical 24 (SSI, USA), a steel reactor with a capacity of 50 ml, and a backpressure regulator BPR (Goregulator, Waters, USA). Each sample was washed with liquid CO_2 for 2 h at a temperature of 20 °C and a pressure of 15 MPa, then the temperature in the reactor was increased to 50 °C and the sample was washed with supercritical CO_2 (15 MPa) for at least 5 h. Then, the pressure in the heated autoclave was gradually (over 30 – 40 min) reduced to atmospheric pressure, after which the autoclave was cooled and opened.

The Bruker D8 Advance X-ray diffractometer (CuKα radiation, Ni filter and Lynxeye detector) was used to identify the phase composition of the products. Diffraction data were collected in the range of 2θ from 7° to 65° with a step of 0.02° and accumulation time of 0.3 s/step. The identification of the diffraction peaks was carried out using the ICDD database. The full-profile analysis of diffraction patterns with quantitative determination of the crystallite sizes was performed using the Rietveld method applied using the MAUD software (version 2.99).

The morphology of the samples was studied by scanning electron microscopy (SEM) at Amber GMH (Tescan, Brno, Czech Republic) or NVision 40 (Carl Zeiss, Oberkochen, Germany) microscope using a secondary electron detector. The SEM images were acquired at acceleration voltage of 1 kV. Energy-dispersive X-ray spectroscopy (EDX) data were obtained using an Ultim Max (Oxford Instruments, Abingdon, UK) detector at an accelerating voltage of 20 kV.

The textural characteristics of the materials were determined by ATX-06 analyzer (Katakon, Russia). The samples were degassed at 80 °C in nitrogen current (1 atm) during 2 hours. The specific surface area was defined with the use of The Brunauer–Emmett–Teller (BET) model, based on 7 points within the range of nitrogen partial pressures (P/P_0) from 0.05 to 0.25.

Diffuse reflection IR spectra were recorded using a laboratory IR Fourier spectrometer FSM 2202 relative to KBr in the range of 400 – 4000 cm^{-1} with a resolution of 2 cm^{-1}, the averaging of 100 spectra was applied. To register the spectra, the samples were diluted in potassium bromide to a weight fraction of 3 %.

Raman spectra were collected using a Confotech NR-500 spectrometer (Sol Instruments), equipped with a 1,800 mm^{-1} grating and a 785 nm laser with 25 mW output power at the sample surface. The ×20 objective lens (NA = 0.55) was used.

Photoluminescence spectra were recorded at room temperature on a Perkin Elmer LS-55 single-beam luminescence spectrometer (resolution 0.5 nm) in the wavelength range from 300 to 800 nm at $\lambda_{\text{em}} = 440$ and 530 nm and at $\lambda_{\text{exc}} = 390$ and 240 nm, the optical slit sizes were 10 nm.

3. Results and discussion

As illustrated in Table 1, the gelation times for the solutions of $GeCl_4$ in acetic acid depended strongly on the molar ratio of acetic acid-to-propylene oxide. Unexpectedly, the higher was the AcOH:PO ratio in the reaction mixture, the lower was the gelation time (see samples Ac20–Ac80 in Table 1). For the mixtures containing AcOH and PO at molar ratios of 2:1 and 8:1, the gelation times differed approximately twofold. Importantly, under the selected experimental conditions, for the reaction mixtures containing germanium chloride, acetic acid and propylene oxide, the gelation time exceeded one week. Addition of an aqueous solution of hydrochloric acid (36.5 wt. %) to the reaction media allowed to obtain lyogels in a several minutes or tens of minutes. Such a significant change in the gelation rate could be induced by free hydroxonium cations which appear upon the addition of strong hydrochloric acid and water and protonate the molecules of propylene oxide due to nucleophilic attack with subsequent triatomic ring opening [43]. Presumably, the rate of these processes in glacial acetic acid is very low due to the low value of the autoprotolysis constant of AcOH which is close to the autoprotolysis constant of water [44].

The appearance of the obtained lyogels is shown in Fig. 2a, all of them were transparent and retained their transparency after the supercritical drying (Fig. 2b), the aerogels possessed extreme fragility and can hardly be handled.

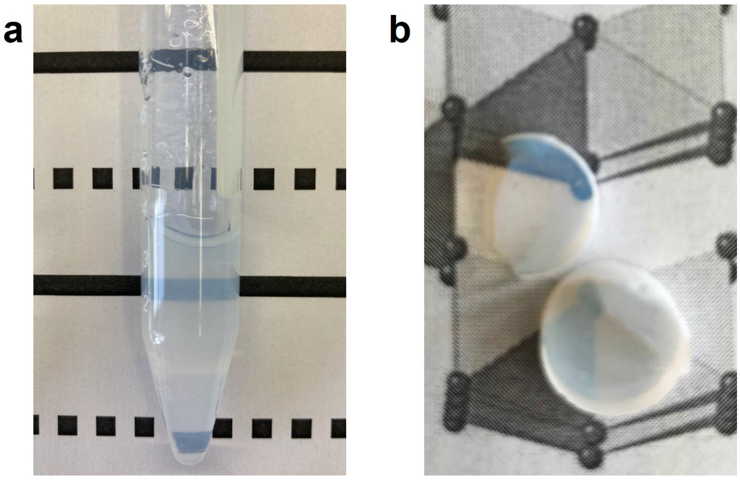

FIG. 2. The visual appearance of the a) germania lyogel formed from $GeCl_4$, acetic acid and propylene oxide as starting reagents (sample Ac60_HCl2.5) and b) the corresponding germania aerogel

According to X-ray diffraction data, the aerogels obtained without the addition of hydrochloric acid in the reaction mixture regardless of the molar content of acetic acid, were amorphous. In contrast, aerogels synthesized in the presence of hydrochloric acid showed diffraction patterns characteristic of hexagonal GeO_2 (Fig. 3). The estimations of crystallite size for the samples Ac60_HCl2.5, Ac60_HCl5, Ac80_HCl5 amounted to 24±2, 20±1 and 20±1 nm, respectively.

Thus, very slow gelation of the solution containing acetic acid, germanium chloride and propylene oxide results in the formation of X-ray amorphous materials while fast gel formation which occurs upon the addition of aqueous HCl to the reaction mixture, results in the formation of nanocrystalline germanium oxide. The exact reasons for such a dramatic

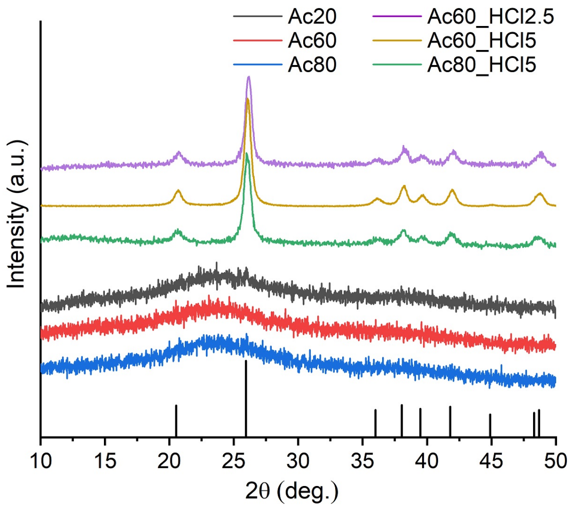

FIG. 3. X-ray diffraction patterns of germania aerogels synthesised from the mixtures of $GeCl_4$, acetic acid and propylene oxide as starting reagents. The Bragg peak positions of GeO_2 (PDF No. 36-1463) are shown as a reference

difference in the structure of GeO_2 aerogels is unclear, they can be related to the very different rates of gelation. One should also consider the chemistry of germanium complexes with acetic acid: their formation and hydrolysis mechanism. Despite the formation of such complexes is discussed in the literature [45] their composition and chemical behavior is underexplored.

IR spectroscopy data for the aerogels are presented in Fig. 4a. All the spectra show two main absorption bands in the region of 1000 – 790 and 620 – 480 cm^{-1}, related to antisymmetric stretching and deformation vibration of Ge–O–Ge in hexagonal GeO_2, correspondingly [46–50]. Absorption band at 755 cm^{-1} can be assigned to the Ge–O stretching vibration, or more probably, to the Ge–OH vibration [32, 51]. The coincidence of the positions and intensity ratios of all the main absorption bands in the IR spectra of amorphous and crystalline samples provides indirect evidence that, in terms of composition, the X-ray amorphous samples also represent germanium dioxide. In the IR spectrum of the Ac60_HCl5 sample in the wavenumber range from 1800 to 1000 cm^{-1}, the most pronounced absorption bands are most likely related to the characteristic vibrations of the acetic acid and propylene oxide molecules [52–54], which remained in the aerogel after supercritical drying. The IR spectroscopy data matched well with the Raman ones (Fig. 4b). The band at 262 cm^{-1} corresponded to the Ge–O bending modes and three bands in range from 440 to 590 cm^{-1} are associated with Ge–Ge stretching motions [55]. Weak peaks in high-frequency region (up to 970 cm^{-1}) are typically assigned to Ge–O stretching motions within tetrahedral GeO_4 groups. Vibrations of the organic residues are manifested in the range above 2800 cm^{-1}. Similar to the IR spectra, the magnitude of these oscillations is most pronounced in the Ac60_HCl5 sample.

From the chemical sense, the mechanism of the formation of germanium oxide through sol-gel route should include the interaction of germanium-containing species with water molecules or hydroxy groups followed by the condensation of germanoles. In the mixtures of $GeCl_4$, glacial acetic acid and propylene oxide one can hardly expect the presence of free water molecules. However, the formation of GeO_2 as a result of interaction of $GeCl_4$ with benzyl alkohols was recently reported [56]. In that case, the formation of water in the reaction mixture was either due to the $GeCl_4$ catalysed interaction of alkohols and the formation of ethers, or due to the alkyl chloride elimination reaction. Thus, it can be expected that the mechanism of GeO_2 formation in glacial acetic acid and propylene oxide can include either the formation of acetic anhydride or, more probably, acetyl chloride.

Note that, according to EDX data, for all the germania aerogels, the presence of chlorine did not exceed 0.1 atomic percent, which indicates that the hydrolysis of germanium tetrachloride occurred quantitatively, and supports the formation of GeO_2.

The microstructure of amorphous samples Ac20, Ac60, Ac80 can be described as a three-dimensional network consisting of nanosized ($\sim$ 20 nm) particles. In turn, crystalline samples (Ac60_HCl2.5, Ac60_HCl5, Ac80_HCl5) consist of micron sized ellipsoid-like aggregates of ultrasmall particles nearly 20 nm in size (Fig. 5). The latter observation is in a good agreement with the results of X-ray diffraction.

Table 2 presents the values of the specific surface area of the obtained aerogels. For the series of amorphous samples, the obtained values are very close to each other ($\sim$ 80 m^2/g), which agrees with the SEM data. Conversely, the specific surface of the crystalline samples differs greatly from each other. The lowest specific surface ($\sim$ 5 m^2/g) was registered for the Ac60_HCl5 sample, which may be due to the presence of the reaction by-products (see the IR spectroscopy

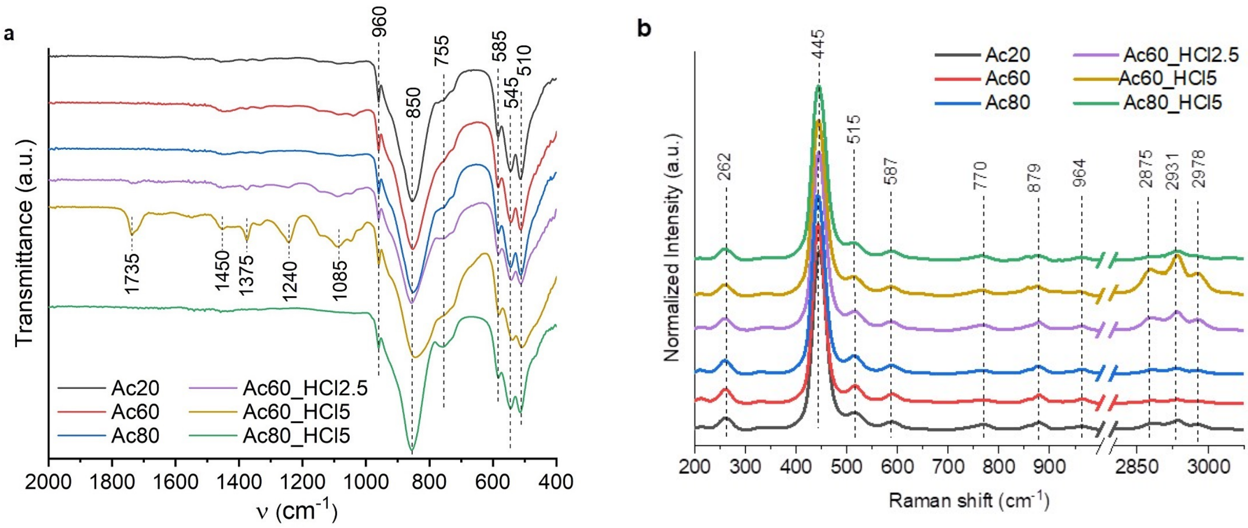

FIG. 4. (a) IR and (b) Raman spectra of germania aerogels synthesised from the mixtures of $GeCl_4$, acetic acid and propylene oxide as starting reagents

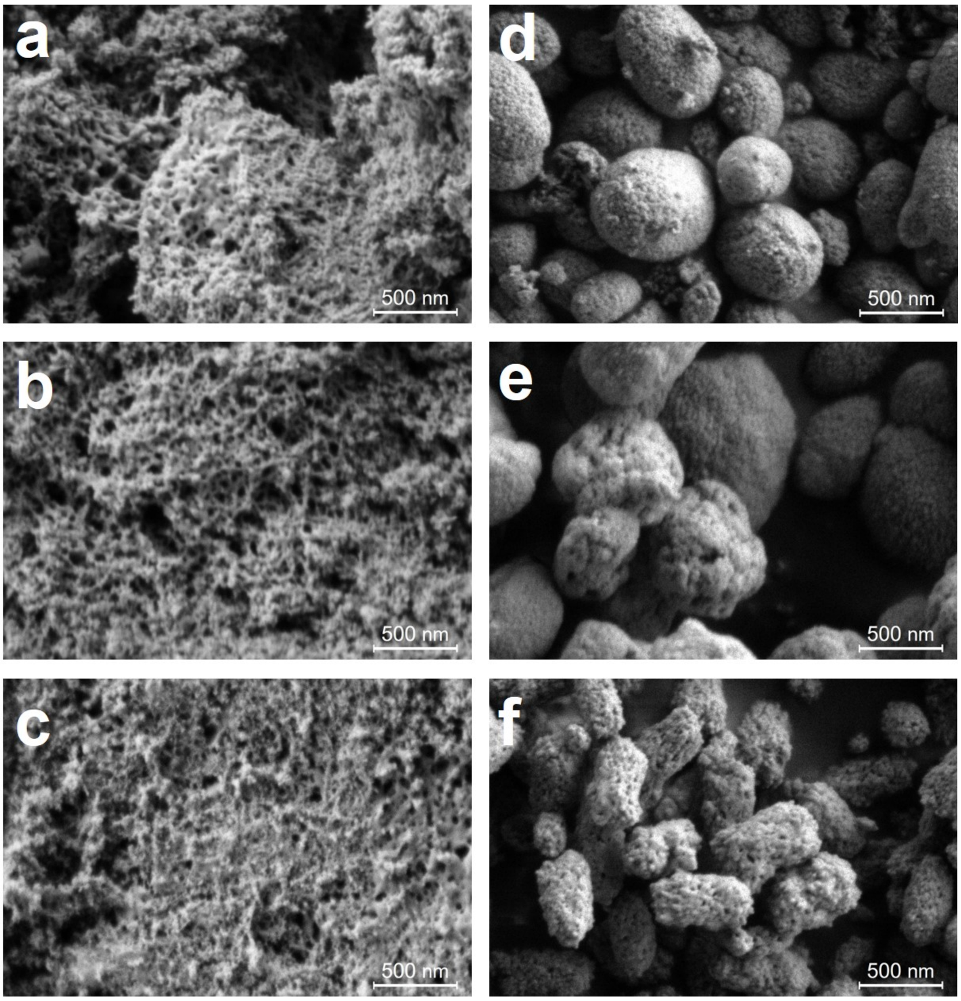

FIG. 5. SEM images of a) Ac20; b) Ac60; c) Ac80; d) Ac60_HCl2.5; e) Ac60_HCl5; f) Ac80_HCl5 samples

data). Despite the fact that, according to SEM data, the Ac60_HCl2.5 sample consists of agglomerates about 500 nm in size, it possessed the largest surface area (~ 113 m^2/g) among all the samples. Probably, the chosen ratio of reagents makes it possible to achieve the most optimal gelation time. The gelation time was low enough to prevent the strong coalescence (ageing) of individual particles, yet high enough for the formation of the 3D aerogel network with reasonable mechanical strength.

Analysis of the luminescent properties has shown that the shape and position of the main bands in the excitation and emission spectra of the obtained aerogels coincide with those for aerogels obtained by both the decomposition of ammonium germanate [50] and the epoxide-induced sol-gel synthesis in an aprotic solvent [36]. The most pronounced bands in the excitation spectra (Fig. 6) recorded at 440 and 530 nm are localized in the region of 238 and 390 nm.

TABLE 2. Specific surface area of germanium dioxide aerogels

Sample	Molar ratio $GeCl_4$:Ac:HCl:Prop	Gel formation duration	S_{BET}, m^2/g
Ac20	1:20:0:10	~20 days	79
Ac60	1:60:0:10	~ 9 days	74
Ac80	1:80:0:10	~ 9 days	83
Ac60_HCl2.5	1:60:2,5:10	~60 min	113
Ac60_HCl5	1:60:5:10	~ 15 min	5
Ac80_HCl5	1:80:5:10	~ 120 min	44

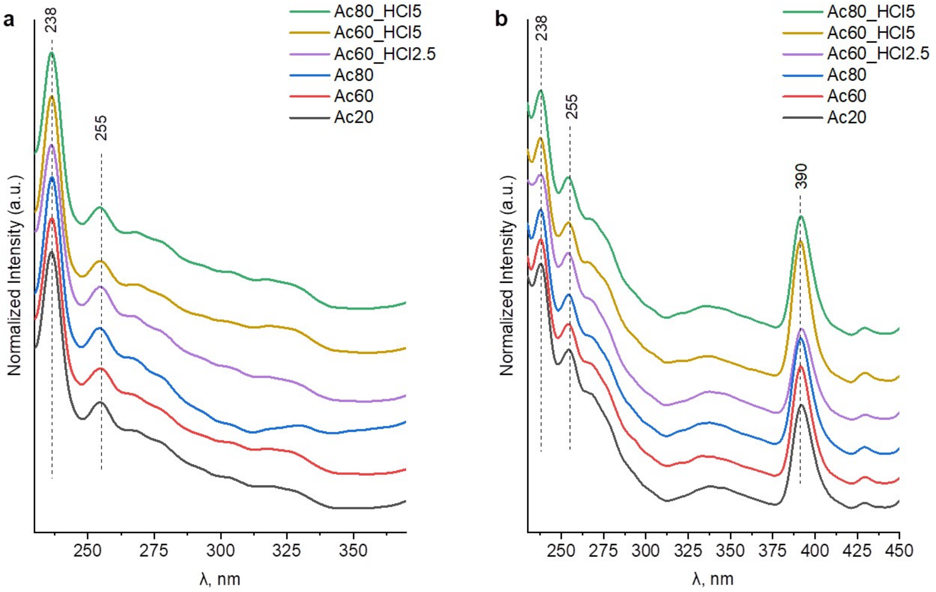

FIG. 6. Excitation spectra recorded at 440 nm (a) and 530 nm (b) of germania aerogels synthesised from the mixtures of $GeCl_4$, acetic acid and propylene oxide as starting reagents

The luminescence spectrum obtained under excitation at 390 nm reveals three well-defined bands in the blue-green spectral range at 447, 487, and 530 nm (Fig. 7a). It is a common point, that the blue and green photoluminescence of GeO_2 powder is associated to radiative recombination processes involving different defects, first of all oxygen and oxygen-germanium vacancies centers [19, 57]. The ratio of the blue and green bands varies for different samples. One plausible explanation for this phenomenon could be attributed to the variation in the number of oxygen vacancies present on the surface of the aerogel materials. When excited by radiation with a higher energy (at 240 nm), the emission spectrum becomes more complex (Fig. 7b). Additional bands appear in the violet region of the spectrum around 370 – 430 nm. The origin of violet photoluminescence is typically ascribed to the presence of neutral oxygen vacancies in germanium oxide [7].

Thus, it has been shown that the use of acetic acid as a solvent for $GeCl_4$ and propylene oxide as a gelation agent leads to the successful formation of monolithic lyogels, in contrast to the previously proposed synthesis with butyl/ethyl acetate,

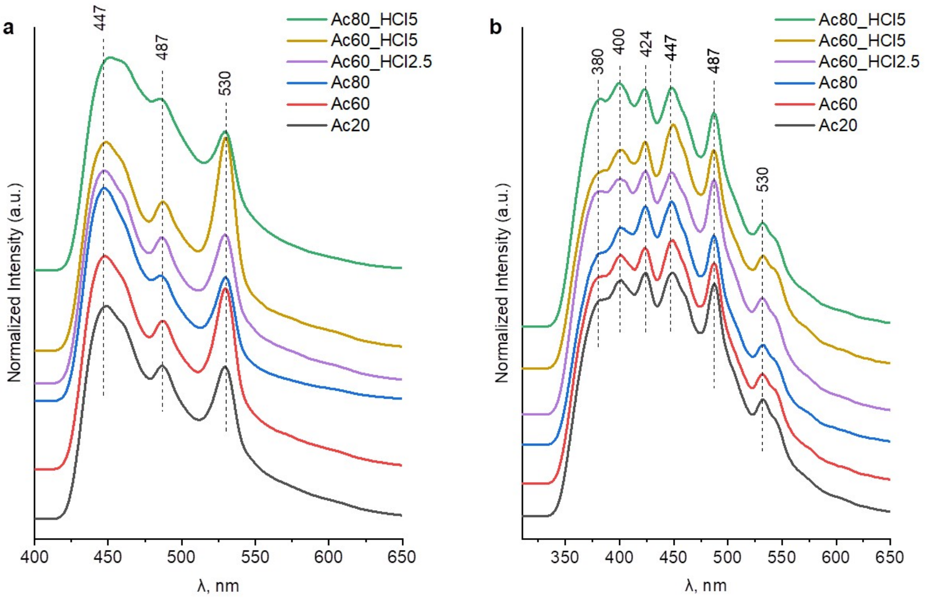

FIG. 7. Emission spectra excited at 390 nm (a) and 240 nm (b) of germania aerogels synthesised from the mixtures of $GeCl_4$, acetic acid and propylene oxide as starting reagents

which also required the use of hydrochloric acid [35, 36]. Although it is evident that the formation of germanium oxide occurs through the non-hydrolytic sol-gel process, further research is needed for establishing the reaction mechanism. Employing supplementary methods, particularly NMR spectroscopic studies of the reaction mixtures at different stages of the gelation process can contribute to understanding of the mechanism. Most importantly, the role of the hydrochloric acid should be elucidated, whether it alters the reaction mechanism or merely accelerates the rate of the reaction. It should be noted that the sol-gel synthesis of crystalline aerogels presents a challenging task for modern materials science [58]. The discovery of the potential to synthesize germanium dioxide aerogels with desired and high textural characteristics through minor alterations of the synthesis route can be a significant advance from a fundamental standpoint. This approach offers the flexibility to tailor the functional properties of the resulting materials, a capability that holds immense promise for diverse applications [59, 60].

4. Conclusions

For the first time, a method for producing germanium dioxide aerogels by the epoxide-induced sol-gel method using acetic acid as a solvent has been proposed. It was found that the molar content of acetic acid used (20-80-fold molar excess relative to $GeCl_4$) has virtually no effect on the composition and microstructure of the products – the resulting aerogels are X-ray amorphous with a particle size of about 20 nm and a specific surface area of about 80 m^2/g. Moreover, the addition of hydrochloric acid to the reaction medium leads to a significantly higher rate of gelation of the initial lyogels and the production of aerogels of crystalline germanium dioxide (hexagonal syngony) with a crystallite size of about 20 nm. The morphology and degree of crystallinity of aerogels did not have a direct impact on their luminescent properties. The general appearance of the excitation and emission spectra was similar for all samples. However, when excited at 390 nm, the ratio of the intensities of the green and blue bands differed between samples.

References

[1] Bioud Y.A., Paradis E., Boucherif A., Drouin D., Arès R. Shape Control of Cathodized Germanium Oxide Nanoparticles. *Electrochem. Commun.*, 2021, **122**, 106906.

[2] Almuslem A.S., Hanna A.N., Yapici T., Wehbe N., Diallo E.M., Kutbee A.T., Bahabry R.R., Hussain M.M. Water Soluble Nano-Scale Transient Material Germanium Oxide for Zero Toxic Waste Based Environmentally Benign Nano-Manufacturing. *Appl. Phys. Lett.*, 2017, **110** (7), 074103.

[3] Simanzhenkov V., Ifeacho P., Wiggers H., Knipping J., Roth P. Synthesis of Germanium Oxide Nanoparticles in Low-Pressure Premixed Flames. *J. Nanosci. Nanotechnol.*, 2004, **4** (1), P. 157–161.

[4] Zhao Q., Lorenz H., Turner S., Lebedev O.I., Van Tendeloo G., Rameshan C., Klötzer B., Konzett J., Penner S. Catalytic Characterization of Pure SnO_2 and GeO_2 in Methanol Steam Reforming. *Appl. Catal. A Gen.*, 2010, **375** (2), P. 188–195.

[5] Kim W.J., Soshnikova V., Markus J., Oh K.H., Anandapadmanaban G., Mathiyalagan R., Perez Z.E.J., Kim Y.J., Yang D.C. Room Temperature Synthesis of Germanium Dioxide Nanorods and Their in Vitro Photocatalytic Application. *Optik (Stuttg).*, 2019, **178**, P. 664–668.

[6] Trukhin A.N. Luminescence of Polymorph Crystalline and Glassy SiO_2, GeO_2: A Short Review. *J. Non. Cryst. Solids*, 2009, **355** (18–21), P. 1013–1019.

[7] Shi R., Zhang R., Chen X., Yang F., Zhao Q., Yu J., Zhao H., Wang L., Liu B., Bao L., Chen Y., Yang H. Controllable Growth of GeO_2 Nanowires with the Cubic and Hexagonal Phases and Their Photoluminescence. *J. Cryst. Growth*, 2011, **336** (1), P. 6–13.

[8] Bose N., Basu M., Mukherjee S. Study of Optical Properties of GeO_2 Nanocrystals as Synthesized by Hydrothermal Technique. *Mater. Res. Bull.*, 2012, **47** (6), P. 1368–1373.

[9] Walker B., Dharmawardhana C.C., Dari N., Rulis P., Ching W.Y. Electronic Structure and Optical Properties of Amorphous GeO_2 in Comparison to Amorphous SiO_2. *J. Non. Cryst. Solids*, 2015, **428**, P. 176–183.

[10] Zhang J., Yu T., Chen J., Liu H., Su D., Tang Z., Xie J., Chen L., Yuan A., Kong Q. Germanium-Based Complex Derived Porous GeO_2 Nanoparticles for Building High Performance Li-Ion Batteries. *Ceram. Int.*, 2018, **44** (1), P. 1127–1133.

[11] Arro C.R., Mohamed A.T.I., Bensalah N. Impact of Ge Content on the Electrochemical Performance of Germanium Oxide/Germanium/ Reduced Graphene (GeO_2/Ge/r-GO) Hybrid Composite Anodes for Lithium-Ion Batteries. *Mater. Today Commun.*, 2022, **30** (January), 103151.

[12] Han L., Wei Q., Chen H., Tang J., Wei M. Open-Framework Germanates Derived GeO_2/C Nanocomposite as a Long-Life and High-Capacity Anode for Lithium-Ion Batteries. *J. Alloys Compd.*, 2021, **881**, 160533.

[13] Mo R., Rooney D., Sun K. Hierarchical Graphene-Scaffolded Mesoporous Germanium Dioxide Nanostructure for High-Performance Flexible Lithium-Ion Batteries. *Energy Storage Mater.*, 2020, **29**, P. 198–206.

[14] Wu Y., Yang P. Germanium Nanowire Growth via Simple Vapor Transport. *Chem. Mater.*, 2000, **12** (3), P. 605–607.

[15] Jiang Z., Xie T., Wang G.Z., Yuan X.Y., Ye C.H., Cai W.P., Meng G.W., Li G.H., Zhang L.D. GeO_2 Nanotubes and Nanorods Synthesized by Vapor Phase Reactions. *Mater. Lett.*, 2005, **59** (4), P. 416–419.

[16] Mathur S., Shen H., Sivakov V., Werner U. Germanium Nanowires and Core-Shell Nanostructures by Chemical Vapor Deposition of $[Ge(C_5H_5)_2]$. *Chem. Mater.*, 2004, **16** (12), P. 2449–2456.

[17] Zhang X., Que W., Chen J., Zhang X., Hu J., Liu W. Concave Micro-Lens Arrays Fabricated from the Photo-Patternable GeO_2/Ormosils Hybrid Sol-Gel Films. *Opt. Mater.*, 2013, **35** (12), P. 2556–2560.

[18] Hsu C.H., Lin J. Sen, He Y. Da, Yang S.F., Yang P.C., Chen W.S. Optical, Electrical Properties and Reproducible Resistance Switching of GeO_2 Thin Films by Sol-Gel Process. *Thin Solid Films*, 2011, **519** (15), P. 5033–5037.

[19] Wu X.C., Song W.H., Zhao B., Sun Y.P., Du J.J. Preparation and Photoluminescence Properties of Crystalline GeO_2 Nanowires. *Chem. Phys. Lett.*, 2001, **349**, P. 210–214.

[20] Zhang Y., Zhu J., Zhang Q., Yan Y., Wang N., Zhang X. Synthesis of GeO_2 Nanorods by Carbon Nanotubes Template. *Chem. Phys. Lett.*, 2000, **317**, P. 504–509.

[21] Krupanidhi S.B., Sayer M., Mansingh A. Electrical Characterization of Amorphous Germanium Dioxide Films. *Thin Solid Films*, 1984, **113** (3), P. 173–184.

[22] Pierre A.C., Pajonk G.M. Chemistry of Aerogels and Their Applications. *Chem. Rev.*, 2002, **102** (11), P. 4243–4266.

[23] Ziegler C., Wolf A., Liu W., Herrmann A., Gaponik N., Eychmüller A. Modern Inorganic Aerogels. *Angew. Chemie Int. Ed.*, 2017, **56** (43), P. 13200–13221.

[24] Feng J., Su B.-L., Xia H., Zhao S., Gao C., Wang L., Ogbeide O., Feng J., Hasan T. Printed Aerogels: Chemistry, Processing, and Applications. *Chem. Soc. Rev.*, 2021, **50** (6), P. 3842–3888.

[25] Gurav J.L., Jung I.K., Park H.H., Kang E.S., Nadargi D.Y. Silica Aerogel: Synthesis and Applications. *J. Nanomater.*, 2010, 2010.

[26] Krishnan V., Gross S., Müller S., Armelao L., Tondello E., Bertagnolli H. Structural Investigations on the Hydrolysis and Condensation Behavior of Pure and Chemically Modified Alkoxides. 2. Germanium Alkoxides. *J. Phys. Chem. B*, 2007, **111** (26), P. 7519–7528.

[27] Livage J., Sanchez C. Sol-Gel Chemistry. *J. Non. Cryst. Solids*, 1992, **145**, P. 11–19.

[28] Shen J., Li Q., Zhou B., Wang J., Chen L. SiO_2-GeO_2 Binary Aerogels with Ultralow Density. *J. Non. Cryst. Solids*, 1997, **220** (1), P. 102–106.

[29] Grandi S., Mustarelli P., Magistris A., Gallorini M., Rizzio E. Synthesis of GeO_2-Doped SiO_2 Aerogels and Xerogels. *J. Non. Cryst. Solids*, 2002, **303** (2), P. 208–217.

[30] Kucheyev S.O., Baumann T.F., Wang Y.M., van Buuren T., Poco J.F., Satcher J.H., Hamza A.V. Monolithic, High Surface Area, Three-Dimensional GeO_2 Nanostructures. *Appl. Phys. Lett.*, 2006, **88** (10), 103117.

[31] Zhang L., Chen G., Chen B., Liu T., Mei Y., Luo X. Monolithic Germanium Oxide Aerogel with the Building Block of Nano-Crystals. *Mater. Lett.*, 2013, **104**, P. 41–43.

[32] Chen G., Chen B., Liu T., Mei Y., Ren H., Bi Y., Luo X., Zhang L. The Synthesis and Characterization of Germanium Oxide Aerogel. *J. Non. Cryst. Solids*, 2012, **358** (23), P. 3322–3326.

[33] Gash A.E., Tillotson T.M., Satcher J.H., Hrubesh L.W., Simpson R.L. New Sol-Gel Synthetic Route to Transition and Main-Group Metal Oxide Aerogels Using Inorganic Salt Precursors. *J. Non. Cryst. Solids*, 2001, **285** (1–3), P. 22–28.

[34] Du A., Zhou B., Zhang Z., Shen J. A Special Material or a New State of Matter: A Review and Reconsideration of the Aerogel. *Materials (Basel).*, 2013, **6** (3), P. 941–968.

[35] Veselova V.O., Kottsov S.Y., Golodukhina S. V., Khvoshchevskaya D.A., Gajtko O.M. Hydrophilic and Hydrophobic: Modified GeO_2 Aerogels by Ambient Pressure Drying. *Nanomaterials*, 2024, **14** (18), 1511.

[36] Gajtko O.M., Golodukhina S. V, Kottsov S.Y., Subcheva E.N., Volkov V.V., Kopitsa G.P., Son A.G., Veselova V.O. Hydrophobic GeO_2 Aerogels by an Epoxide-Induced Process. *Gels*, 2025, **11** (4), 225.

[37] Stöcker C., Baiker A. Zirconia Aerogels: Effect of Acid-to-Alkoxide Ratio, Alcoholic Solvent and Supercritical Drying Method on Structural Properties. *J. Non. Cryst. Solids*, 1998, **223** (3), P. 165–178.

[38] Aguado-Serrano J., Rojas-Cervantes M.L. Titania Aerogels. M*icroporous Mesoporous Mater.*, 2006, **88** (1–3), P. 205–213.

[39] Dong W., Yen S., Paik J., Sakamoto J. The Role of Acetic Acid and Glycerol in the Synthesis of Amorphous MgO Aerogels. *J. Am. Ceram. Soc.*, 2009, **92** (5), P. 1011–1016.

[40] Poco J., Satcher J., Hrubesh L. Synthesis of High Porosity, Monolithic Alumina Aerogels. *J. Non. Cryst. Solids*, 2001, **285** (1–3), P. 57–63.

[41] Shimoyama Y., Ogata Y., Ishibashi R., Iwai Y. Drying Processes for Preparation of Titania Aerogel Using Supercritical Carbon Dioxide. *Chem. Eng. Res. Des.*, 2010, **88** (10), P. 1427–1431.

[42] Sui R., Rizkalla A.S., Charpentier P.A. Synthesis and Formation of Silica Aerogel Particles By a Novel Sol-Gel Route in Supercritical Carbon Dioxide. *J. Phys. Chem. B*, 2004, **108** (32), P. 11886–11892.

[43] Baumann T.F., Gash A.E., Satcher J.H. A Robust Approach to Inorganic Aerogels: The Use of Epoxides in Sol–Gel Synthesis. *Aerogels Handb.*, 2011, P. 155–170.

[44] Rondinini S., Longhi P., Mussini P.R., Mussini T. Autoprotolysis Constants in Nonaqueous Solvents and Aqueous Organic Solvent Mixtures. *Pure Appl. Chem.*, 1987, **59** (12), P. 1693–1702.

[45] Pokrovski G.S., Schott J. Experimental Study of the Complexation of Silicon and Germanium with Aqueous Organic Species: Implications for Germanium and Silicon Transport and Ge/Si Ratio in Natural Waters. *Geochim. Cosmochim. Acta*, 1998, **62** (21–22), P. 3413–3428.

[46] Lobaz V., Rabyk M., Pánek J., Doris E., Nallet F., Štěpánek P., Hrubý M. Photoluminescent Polysaccharide-Coated Germanium(IV) Oxide Nanoparticles. *Colloid Polym. Sci.*, 2016, **294** (7), P. 1225–1235.

[47] Javadi M., Yang Z., Veinot J.G.C. Surfactant-Free Synthesis of GeO_2 Nanocrystals with Controlled Morphologies. *Chemical Communications*, 2014, **50** (46), P. 6101–6104.

[48] Micoulaut M., Cormier L., Henderson G.S. The Structure of Amorphous, Crystalline and Liquid GeO_2. *J. Phys. Condens. Matter*, 2006, **18** (45), R753–R784.

[49] Błaszczak K., Adamczyk A., Wędzikowska M., Rokita M. Infrared Studies of Devitrification Li_2O – B_2O_3–$2GeO_2$ Glass. *J. Mol. Struct.*, 2004, **704** (1–3), P. 275–279.

[50] Veselova V.O., Khvoshchevskaya D.A., Golodukhina S. V., Kottsov S.Y., Gajtko O.M. One Simple Approach to Novel Germania and Germanate Aerogels. *Microporous Mesoporous Mater.*, 2024, **379**, 113282.

[51] Kawai T., Usui Y., Kon-No K. Synthesis and Growth Mechanism of GeO_2 Particles in AOT Reversed Micelles. *Colloids Surfaces A Physicochem. Eng. Asp.*, 1999, **149** (1–3), P. 39–47.

[52] Gofurov S., Makhmanov U., Kokhkharov A., Ismailova O.B. Structural and Optical Characteristics of Aqueous Solutions of Acetic Acid. *Appl. Spectrosc.*, 2019, **73** (5), P. 503–510.

[53] Hasan M.A., Zaki M.I., Pasupulety L. Oxide-Catalyzed Conversion of Acetic Acid into Acetone: An FTIR Spectroscopic Investigation. *Appl. Catal. A Gen.*, 2003, **243** (1), P. 81–92.

[54] Hudson R.L., Loeffler M.J., Yocum K.M. Laboratory Investigations into the Spectra and Origin of Propylene Oxide: A Chiral Interstellar Molecule. *Astrophys. J.*, 2017, **835** (2), 225.

[55] Madon M., Gillet P., Julien C., Price G.D. A Vibrational Study of Phase Transitions among the GeO_2 Polymorphs. *Phys. Chem. Miner.*, 1991, **18** (1), P. 7–18.

[56] Kitschke P., Schulze S., Hietschold M., Mehring M. Synthesis of Germanium Dioxide Nanoparticles in Benzyl Alcohols – a Comparison. *Main Gr. Met. Chem.*, 2013, **36** (5–6).

[57] Bose N., Basu M., Mukherjee S. Study of Optical Properties of GeO_2 Nanocrystals as Synthesized by Hydrothermal Technique. *Mater. Res. Bull.*, 2012, **47** (6), P. 1368–1373.

[58] Takemoto M., Tokudome Y., Noguchi D., Ueoka R., Kanamori K., Okada K., Murata H., Nakahira A., Takahashi M. Synthesis of a Crystalline and Transparent Aerogel Composed of Ni–Al Layered Double Hydroxide Nanoparticles through Crystallization from Amorphous Hydrogel. *Langmuir*, 2020, **36** (32), P. 9436–9442.

[59] Khan I., Saeed K., Khan I. Nanoparticles: Properties, Applications and Toxicities. *Arab. J. Chem.*, 2019, **12** (7), P. 908–931.

[60] Tretyakov Y.D., Goodilin E.A. Key Trends in Basic and Application-Oriented Research on Nanomaterials. *Russ. Chem. Rev.*, 2009, **78** (9), P. 801–820.

Submitted 24 January 2025; revised 28 March 2025; accepted 5 May 2025

Information about the authors:

Olga M. Gajtko – Kurnakov Institute of General and Inorganic Chemistry of the Russian Academy of Sciences, Moscow, Russia; ORCID 0000-0001-6424-1282; olga.gajtko@igic.ras.ru

Svetlana V. Golodukhina – Kurnakov Institute of General and Inorganic Chemistry of the Russian Academy of Sciences, Moscow, Russia; ORCID 0000-0001-9317-1340; golodukhina@igic.ras.ru

Sergey Yu. Kottsov – Kurnakov Institute of General and Inorganic Chemistry of the Russian Academy of Sciences, Moscow, Russia; ORCID 0000-0001-8263-889X; skottsov@igic.ras.ru

Alexandra G. Son – Kurnakov Institute of General and Inorganic Chemistry of the Russian Academy of Sciences, Moscow, Russia; ORCID 0009-0006-7107-5714; agson@igic.ras.ru

Taisiya O. Kozlova – Kurnakov Institute of General and Inorganic Chemistry of the Russian Academy of Sciences, Moscow, Russia; ORCID 0000-0002-9757-9148; taisiya@igic.ras.ru

Alexander E. Baranchikov – Kurnakov Institute of General and Inorganic Chemistry of the Russian Academy of Sciences, Moscow, Russia; ORCID 0000-0002-2378-7446; baranchikov@igic.ras.ru

Conflict of interest: the authors declare no conflict of interest.